Journal of Alloys and Compounds 874 (2021) 159858

Contents lists available at ScienceDirect

Journal of Alloys and Compounds

journal homepage: www.elsevier.com/locate/jalcom

Electrochemical preparation of $Ni(OH)_2$/CoOOH bilayer films for application in energy storage devices

L. Aguilera[a], Y. Leyet[b,*], A. Almeida[c], J. Agostinho Moreira[c], J. Pérez de la Cruz[d], Erix A. Milán-Garcés[e], R.R. Passos[a], L.A. Pocrifka[a]

[a] University Federal of Amazonas, Department of Chemistry, Manaus, AM, Brazil
[b] University Federal of Amazonas, Department of Materials Engineering, Manaus, AM, Brazil
[c] IFIMUP-IN, Institute of Nanoscience and Nanotechnology, Department of Physics and Astronomy, Faculty of Sciences of the University of Porto, 4169-007 Porto, Portugal
[d] ISQ, Instituto de soldadura e qualidade, Av. Prof. Dr. Cavaco Silva, 2740-120 Porto, Portugal
[e] Instituto de Física, Universidade de São Paulo, Rua do Matão 1371, 05508090 São Paulo, SP, Brazil

ARTICLE INFO

Article history:
Received 13 January 2021
Received in revised form 8 March 2021
Accepted 5 April 2021
Available online 9 April 2021

Keywords:
Bilayer films
Nickel hydroxide
Cobalt oxyhydroxide
Electrodeposition

ABSTRACT

CoOOH/$Ni(OH)_2$ and $Ni(OH)_2$/CoOOH bilayer films were obtained through electrochemical deposition of $Ni(OH)_2$ and $Co(OH)_2$ single layers onto steel plate substrate, with subsequent electrochemical oxidation of $Co(OH)_2$ to form CoOOH. The films were structurally characterized using X-ray diffraction and Raman spectroscopy techniques. Cyclic voltammetry, galvanostatic charge-discharge and electrochemical impedance spectroscopy techniques were used to perform the electrochemical characterization of the prepared bilayers. It was verified that during the electrochemical oxidation, CoOOH formation occurs without $Ni(OH)_2$ oxidation. $Ni(OH)_2$ films deposited on CoOOH (CoOOH/$Ni(OH)_2$) showed a superior electrochemical performance, with 324.27 mA h g^{-1} and 96.82% at 1.0 mA cm^{-2} for the specific capacity and capacity retention respectively. It was also determined that the relaxation time constant under this condition is 17.05 s. These results suggested that the CoOOH/$Ni(OH)_2$ bilayer films might be potential candidates for application as electrode in energy storage devices.

1. Introduction

In the persistent race of the scientific community for finding efficient electrode materials with applications in hybrid supercapacitors, transition metal hydroxides have been catalogued as very attractive candidates. This is largely due to their high specific capacitances, resulting from redox reactions with hydroxyl anions in alkaline electrolytes. In comparison to other metal oxides, the high redox activity of transition metal hydroxides is associated with their lamellar structure, which facilitates ions diffusion from the electrolyte to the bulk, making the charge storage process less dependent on the material surface area [1]. Among the transition metal hydroxides, nickel hydroxide ($Ni(OH)_2$) has been recognized as the most attractive, due to its simple synthesis method, excellent electrochemical properties, high capacitance values and low production cost [2–4]. It has been suggested that the pseudo-capacitive properties of $Ni(OH)_2$ in its nanostructured form might arise due to the decrease of diffusion distances and ions reversible intercalation in the structure [5,6]. In this case, the total capacitance measured value might result from pseudo-capacitive contributions, the double electric layer and the faradaic reactions from the ions intercalation. Their suitable combination might lead to high energy and power densities, being a great motivation for the development and study of $Ni(OH)_2$ composites in the nanostructured form. On the other hand, it has been reported that $Ni(OH)_2$ suffer of low conductivity and that it is frequently obtained in an agglomerate form, hindering the electrolyte ions diffusion into the material structure, which compromise its electrochemical performance.

Most of the actual studies refer to the search for new synthetic routes to obtain $Ni(OH)_2$ in its nanoparticle and non-agglomerated forms and composites by mixing with carbon or other metal oxides. The aim of these approaches is to improve the conductivity of suitable electrodes of $Ni(OH)_2$ for applications that require high energy and power densities [7]. Among the most used materials for that purpose, it could be found the oxidized cobalt phases (oxides and oxyhydroxides) [8–11]. For a long time, cobalt oxides have been

* Corresponding author.
E-mail address: yurileyet@yahoo.es (Y. Leyet).

https://doi.org/10.1016/j.jallcom.2021.159858
0925-8388/

extensively used as additives in nickel-cadmium and nickel-metal hydride batteries [12,13].

The main methods of obtaining cobalt oxides and oxyhydroxides involve reactions in a basic medium with the presence of a strong oxidant, where cobalt hydroxide (α or β) is usually used as a precursor. Oxidation of alpha cobalt hydroxide (α-$Co(OH)_2$) produces non-stoichiometric γ-CoOOH, which shows higher electrochemical performance than the other cobalt hydroxide phases. This is associated to the Co^{4+} ions in the γ-CoOOH structure, which greatly improves its conductivity [9]. One disadvantage in the use of alpha cobalt hydroxide is associated with its instability during the synthesis process, which generally present a turbostratic structure that rapidly transforms to a β-$Co(OH)_2$ phase by expulsion of the inserted anions between the material lamella.

An attractive solution to this problem is the production of lamellar or double layered hydroxides structures. Special attention has been given to nickel and cobalt hydroxides bilayer structures. Most of the studies involving Ni and Co hydroxides are focused on their synergistic action, in comparison with the simple hydroxides, by combining the redox response of the Ni^{2+}/Ni^{3+} and Co^{2+}/Co^{3+} pairs [1,14–18]. However, these materials still have some disadvantages that include the use of active materials and capacity values far below from the expected theoretical limits. What seems to be the most viable way to solve these difficulties is the rational design of materials. Obtaining heterostructures, such as core-shell or layered films can be effective approaches to combine the properties of these hydroxides.

In the present work, electrodeposition method was used for the synthesis of CoOOH/$Ni(OH)_2$ and $Ni(OH)_2$/CoOOH bilayer films, grown directly onto stainless steel substrates. Their lattice dynamics and electrochemical behavior were experimentally studied by using Raman spectroscopy, Cyclic Voltammetry, Galvanostatic Charge-Discharge, and Electrochemical Impedance Spectroscopy. The Raman data were analyzed and compared with the results obtained by the other techniques. The specific capacity and time constant of the films were also determined. A critical evaluation of the results was carried out and the possibility of using these films as electrode materials with higher performance was discussed.

2. Experimental

2.1. Synthesis of the bilayer films

All chemicals used in the reactions had analytical grade and were used without further purification (Sigma-Aldrich). Milli-Q water was used during all procedures. The steel plate substrates were cleaned by sandblast followed by rinsing with Milli-Q water as well.

The CoOOH/$Ni(OH)_2$ and $Ni(OH)_2$/CoOOH bilayer films were obtained following the scheme shown in Fig. 1. The electrodeposition was implemented in a standard three-electrode glass cell with a clean steel plate substrate as working electrode. A platinum plate and an Ag/AgCl were the counter and reference electrode, respectively. All the steps were carried out at room temperature.

2.1.1. Preparation of nickel hydroxide deposited on cobalt oxyhydroxide (CoOOH/$Ni(OH)_2$) films

The cobalt hydroxide film was initially electrodeposited from 0.025 mol L^{-1} $CoCl_2{\cdot}6H_2O$ and $Co(NO_3)_2{\cdot}6H_2O$ aqueous electrolytes in proportion 1:1 using a potentiostatic mode (potential of −1.0 V) for 10 min. Thereafter, nickel hydroxide film was electrodeposited onto the $Co(OH)_2$ film from a 0.1 mol L^{-1} $NiSO_4{\cdot}6H_2O$ aqueous electrolyte using a galvanostatic mode (current density of −2.0 mA cm^{-2}) for 30 min. Then, the electrochemical oxidation of $Co(OH)_2$ to form CoOOH was performed in 1 mol L^{-1} KOH through successive cycles of cyclic voltammetry (10 cycles) at 10 mV s^{-1} in the potential range of −0.2–0.5 V. The synthesized bilayer films were carefully rinsed several times with Milli-Q water, and finally dried in air.

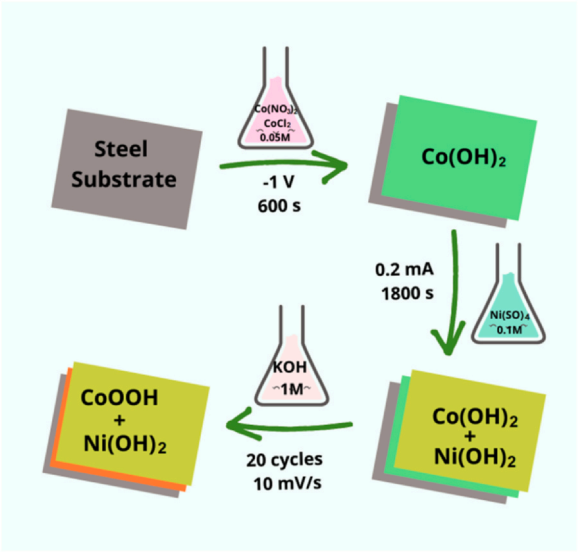

Fig. 1. Scheme for obtaining CoOOH/$Ni(OH)_2$ bilayer films.

2.1.2. Preparation of cobalt oxyhydroxide deposited on nickel hydroxide ($Ni(OH)_2$/CoOOH) films

Similar conditions were used for the case of CoOOH/$Ni(OH)_2$ films but reversing the steps. The approximate mass of both bilayer films (CoOOH/$Ni(OH)_2$ and $Ni(OH)_2$/CoOOH) was 0.0019 g.

2.2. Microstructural, Lattice dynamics and electrochemical characterization

X-Ray Diffraction (XRD) data were obtaining by using a Philips X′Pert diffractrometer based on a Bragg–Brentano para-focusing optics configuration operating with Cu-Kα radiation at 30 mA and 40 kV.

Micro-Raman measurements were carried out with a LABRAM system from Jobin-Yvon. The laser excitation wavelength was 524 nm with a power of 30 mW. The samples were placed under the objective of a microscope and the Raman scattered light was focused on the spectrometer slit using a 180° scattering geometry. The investigated area was 1 mm^2 and the spectra were recorded between 100 and 1200 cm^{-1} with an integration time of 60 s

The electrochemical characterization of the bilayer films was performed using Cyclic Voltammetry (CV), Galvanostatic Charge-Discharge (GCD) and Electrochemical Impedance Spectroscopy (EIS) techniques. Initially, the voltamograms of $Ni(OH)_2$/CoOOH and CoOOH/$Ni(OH)_2$ bilayer films were obtained in the corresponding potential window and at different scan rate with the aim of study the electrochemical activity of the materials. For this analysis, the film prepared on the substrate was used as the working electrode, a platinum plate as the counter electrode, and Ag/AgCl/saturated KCl as the reference electrode. A solution of 1.0 mol L^{-1} KOH was the electrolyte solution. Cyclic voltammograms were acquired in a −0.2 and 0.6 V potential range and different scan rates, while the GCD cycles were recorded within a −0.2 and 0.45 V potential window at different current densities. The electrochemical impedance spectra (frequency range from 0.1 to 10^4 Hz) were collected with an Open Circuit Potential (OCP). All measurements were conducted by using an Autolab Potentiostat (PGSTAT 302N).

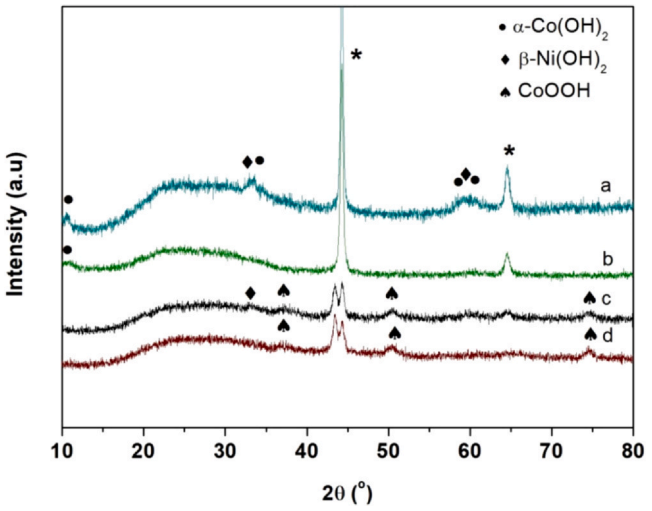

Fig. 2. X-ray diffraction patterns for bilayer films: (a) $Co(OH)_2/Ni(OH)_2$, (b) $Ni(OH)_2/Co(OH)_2$, (c) $CoOOH/Ni(OH)_2$ and (d)$Ni(OH)_2/CoOOH$.

3. Results and discussion

3.1. Structural characterization

The X-ray diffraction patterns of the $Co(OH)_2/Ni(OH)_2$ and $Ni(OH)_2/Co(OH)_2$ bilayer films obtained before and after electrochemical oxidation are shown in Fig. 2. In the absence of oxidation the Bragg peaks are observed at 2θ = 10.49°, 34.38°, 58.40° and 60.70° (Fig. 2a and b) and can be assigned to the plans (003), (009), (110) and (113) of the α-$Co(OH)_2$ hexagonal phase (JCPDS No- 46-0605). The peaks at 2θ = 33.30° and 59.21° correspond to the plans (100) and (110) of the β-$Ni(OH)_2$ hexagonal phase (JCPDS No- 14-0117). Upon electrochemical oxidation the diffraction peaks occur at 2θ = 37.23°, 50.38° and 74.70° (see Fig. 2c and d). They can be indexed to the planes (012), (015) and (202) of γ-CoOOH phase (JCPDS No- 73-0497) with rhombohedral structure. Some peaks corresponding to β-Ni $(OH)_2$ were also observed. These facts confirmed the oxidation of α-Co $(OH)_2$ to form γ-CoOOH and the absence of the oxidation of β-$Ni(OH)_2$.

3.2. Characterization by Raman spectroscopy

Unpolarized micro-Raman spectra of the prepared films, collected at room temperature, are shown in Fig. 3. The $Ni(OH)_2$ and $Co(OH)_2$ single films Raman spectra (see Fig. 3a) exhibit the pure Ni and Co hydroxides representative bands, without any Ni or Co oxide or oxyhydroxide formation. Concerning to the $Co(OH)_2$ spectrum, six bands could be observed at 473 cm^{-1}, 616 cm^{-1}, 845 cm^{-1}, 984 cm^{-1} 1044 cm^{-1} and 1126 cm^{-1}. The Raman profile agree with those published for the α-$Co(OH)_2$ phase [19,20]. The $Ni(OH)_2$ film Raman spectrum exhibits a richer profile, with different bands, observed at 273 cm^{-1}, 457 cm^{-1}, 522 cm^{-1}, 692 cm^{-1}, 845 cm^{-1}, 984 cm^{-1}, 1044 cm^{-1} and 1126 cm^{-1}. The most prominent band is located at 522 cm^{-1}. Based on the work of Hall et. al. [21], the relatively wideness of these bands is an evidence of the low crystallinity degree of the films. The other bands observed in this spectrum are compatible with those reported for the β-$Ni(OH)_2$ phase.

The Raman spectrum of the $Co(OH)_2/Ni(OH)_2$ bilayer films, without oxidation, is presented in Fig. 3b). The Raman bands frequencies observed of the metal hydroxide bilayer films agree with those reported for the simple hydroxide compounds. In this work, the assignment mode of the main Raman bands is based on the current literature [19–23]. The OMeO (Me= Co, Ni) bending mode is observed at 466 cm^{-1} [19], while the intense band at 521 cm^{-1} is

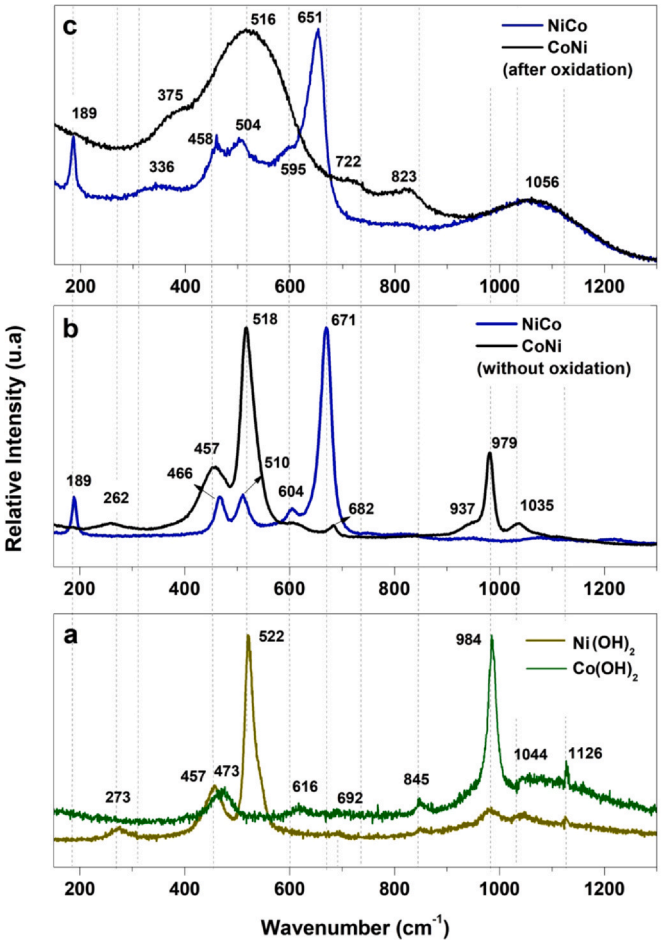

Fig. 3. Raman spectrum of the $Ni(OH)_2$ and $Co(OH)_2$ simple hydroxides (a), $Co(OH)_2/Ni(OH)_2$ bilayer films without oxidation (b), and after oxidation (c).

assigned to the symmetrical stretching mode MeO [19,20]. As above-mentioned, the wideness of these bands is an evidence of the low crystallization degree of the bilayer films. The typical band assigned to Ni or Co hydroxides vibration is located 617 cm^{-1} [22,23], while the O-H vibrations are observed at 937 cm^{-1}, 979 cm^{-1} and 1035 cm^{-1} [19]. It is observed in the literature [21,23], certain divergences with respect to the bands reported for each material and its position, since they are strongly dependent on which structure is being analyzed as result of the material polymorphism. Small shifts in the frequency of the internal vibrational modes might be also caused by mechanical stress within the crystal [21]. Additional Raman peaks in the network vibration region have been attributed to structural defects, proton vacancies and chemical impurities (for example, sulfate derived from synthesis) [23].

The Raman spectrum of the bilayer films after the electrochemical oxidation is shown in Fig. 3c). The widened nature of the bands in CoNi films after the oxidation process does not allow to determine their exact position. However, bands at 375 cm^{-1}, 722 cm^{-1} and 823 cm^{-1} can be observed, which are characteristic of the CoOOH phase [19,20]. On the other hand, in NiCo films the Raman spectrum shows bands at 189 cm^{-1}, 336 cm^{-1}, 458 cm^{-1}, 504 cm^{-1}, 595 cm^{-1}, 651 cm^{-1} and a wide band centered on 1056 cm^{-1}. Bands located at 458 cm^{-1} and 651 cm^{-1} are assigned to the nickel hydroxide phase, which does not experiment oxidation under the conditions studied. However, these bands have small relative intensity than those found in the Raman spectra of films without oxidizing. Be aware that the bands located at 336 cm^{-1}, 504 cm^{-1}, 595 $cm^{-1}$and 1056 cm^{-1} show a clear evidence for the

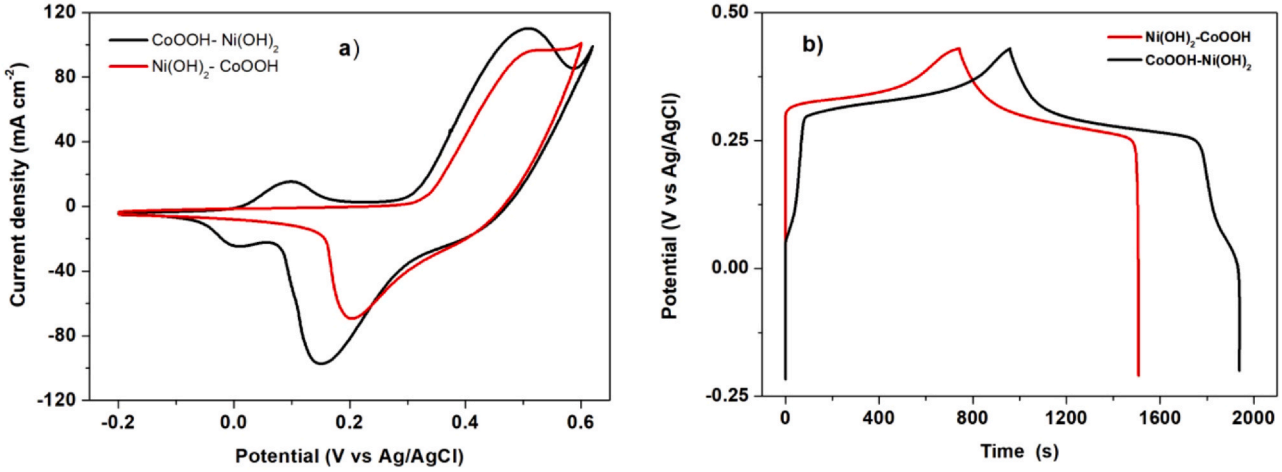

Fig. 4. Voltamograms of CoOOH/$Ni(OH)_2$ and $Ni(OH)_2$/CoOOH bilayer films (scan rate of 20 mV s^{-1}) (a) and Galvanostatic Charge-Discharge Curves of CoOOH/$Ni(OH)_2$ and $Ni(OH)_2$/CoOOH bilayer films (current density of 1.0 mA cm^{-2}) (b).

presence of CoOOH phase in the bilayer films after electrochemical oxidation [19,20]. Finally, the band at 189 cm^{-1} could not be assigned to either nickel hydroxide or cobalt oxyhydroxide and it can be associated to a residual Co_3O_4 phase that might appear due to a possible oxidation of the CoOOH phase during the electrochemical oxidation process [24].

3.3. Electrochemical characterization

The voltammograms of the films are shown in Fig. 4(a). The CV curves of the CoOOH/$Ni(OH)_2$ films show the formation of two pairs of redox peaks, which occur approximately at the same potentials of the redox response of pure $Ni(OH)_2$ and CoOOH components (see Fig. S1- Supporting Information). This indicates that both layers contribute to the redox performance of the film. The specific current of the redox reaction of Co in the bilayer film is lower than that observed in the CoOOH single film, probably due to the formation of the thin internal layer. In turn, the specific current of the redox reaction of Ni increases in comparison to $Ni(OH)_2$ films. This behavior might occur due to the formation of thin $Ni(OH)_2$ particles distributed over the CoOOH sheets, which somehow produces an increase of the active sites of the material. Contrarily, in the $Ni(OH)_2$/CoOOH films, only the formation of a pair of redox peaks at the simple $Ni(OH)_2$ position is observed, but the response of the specific current in the peaks is greater than that obtained in single $Ni(OH)_2$ films, evidencing the contribution from the CoOOH layer. The $Ni(OH)_2$/CoOOH lower response, when compared to the CoOOH/$Ni(OH)_2$ bilayers might be associated to the decrease in conductivity between the current-collecting substrate film caused by the $Ni(OH)_2$. In addition, it can be observed that the potential window corresponding to the CoOOH/$Ni(OH)_2$ film is higher than those obtained for the other materials, which is very encouraging for applications in energy storage devices.

To determine the specific capacitance values of the bilayer films, GCD measurements were performed and the obtained results are shown in Fig. 4(b). The GCD curve of the CoOOH/$Ni(OH)_2$ bilayers shows the presence of two levels, corresponding to the combine response of both redox reactions. In the case of other films, the curves only show a plateau. The range of potential in which the films present electrochemical response can also be determined from the GCD curves. As in the CV analysis, the CoOOH/$Ni(OH)_2$ bilayers respond in a larger scale than that observed for simple films (Fig. S2- Supporting Information). The calculated values of the specific capacity for the CoOOH/$Ni(OH)_2$ and $Ni(OH)_2$/CoOOH bilayers at 1.0 mA cm^{-2} are 324.27 mA h g^{-1} (1795 Fg^{-1}) and 237.35 mA h g^{-1} (1314 Fg^{-1}), respectively. The higher values for the CoOOH/$Ni(OH)_2$ bilayers can be somehow associated to the greater contribution from higher number of active sites of the electroactive $Ni(OH)_2$ deposited on the CoOOH film. This result clearly demonstrates the advantage of combining multiple redox reactions to obtain new materials with potential applications in energy storage.

To better understand the electrochemical behavior of the CoOOH/$Ni(OH)_2$ bilayers, a cyclic voltammetry study was carried out at different scanning speeds, as shown in Fig. 5(a). The profiles show a displacement of the redox peaks and an increment in the specific current with the increase in the scan speed, indicating that the redox reactions are almost of reversible nature. The electrodes polarization at higher scan rate results in an increase in the potential difference between the anode and cathode peaks. The conservation of voltammogram shapes indicates easy OH^- ions transport across the bilayers, possibly due to the lamellar structure of the prepared materials that facilitates the ions diffusion. Fig. 5b) shows the dependence of the current anode and cathode peaks versus the square root of the scan rate. As can be seen, there is a linear dependence for the two pairs of oxy-reduction peaks. This indicated that the reactions occurring in the material are diffusion controlled processes.

The charge storage with the increase of the current constitutes a relevant parameter in the material applicability, since it determines its performance capacity. Fig. 5(c) shows the GCD curves of the CoOOH/$Ni(OH)_2$ bilayers when the current density increases from 1.0 mA cm^{-2} to 10 mA cm^{-2}. Fig. 5(d) shows the variation of the capacitance with respect to the current density and the retention percentage. The calculated values of specific capacity change from 324.27 mA h g^{-1} (1795 F g^{-1}) at 1.0 mA cm^{-2} to 313.79 mA h g^{-1} (1738 F g^{-1}) at 10 mA cm^{-2}, as shown in Fig. 5d). The high percentage of retention capacitance is remarkable, when the current density increases tenfold of its value. For 10 mA cm^{-2}, 96.82% of the retention capacitance is reached, indicating good charge storage capacity at higher charge-discharge rates. Another important parameter in the performance of the material is the stability as a function of the number of charge-discharged cycles. In this case, a capacity retention of 87.96% was achieved after 1500 cycles, as shown in Fig. 5(e).

These results are comparable with those found by previous studies using other types of bilayer films [1,14,15]. For example, Zheng et al. [14] studied multilayer films with different combinations of CoOOH and MnO_2. They obtained the best results for films where the first layer of CoOOH and the second layer of MnO_2. In these cases, the CoOOH was first electrodeposited on indium-tin oxide (ITO) substrate. Then, the films were placed in a solution with exfoliated nanosheet of MnO_2, which allowed their deposition on the CoOOH

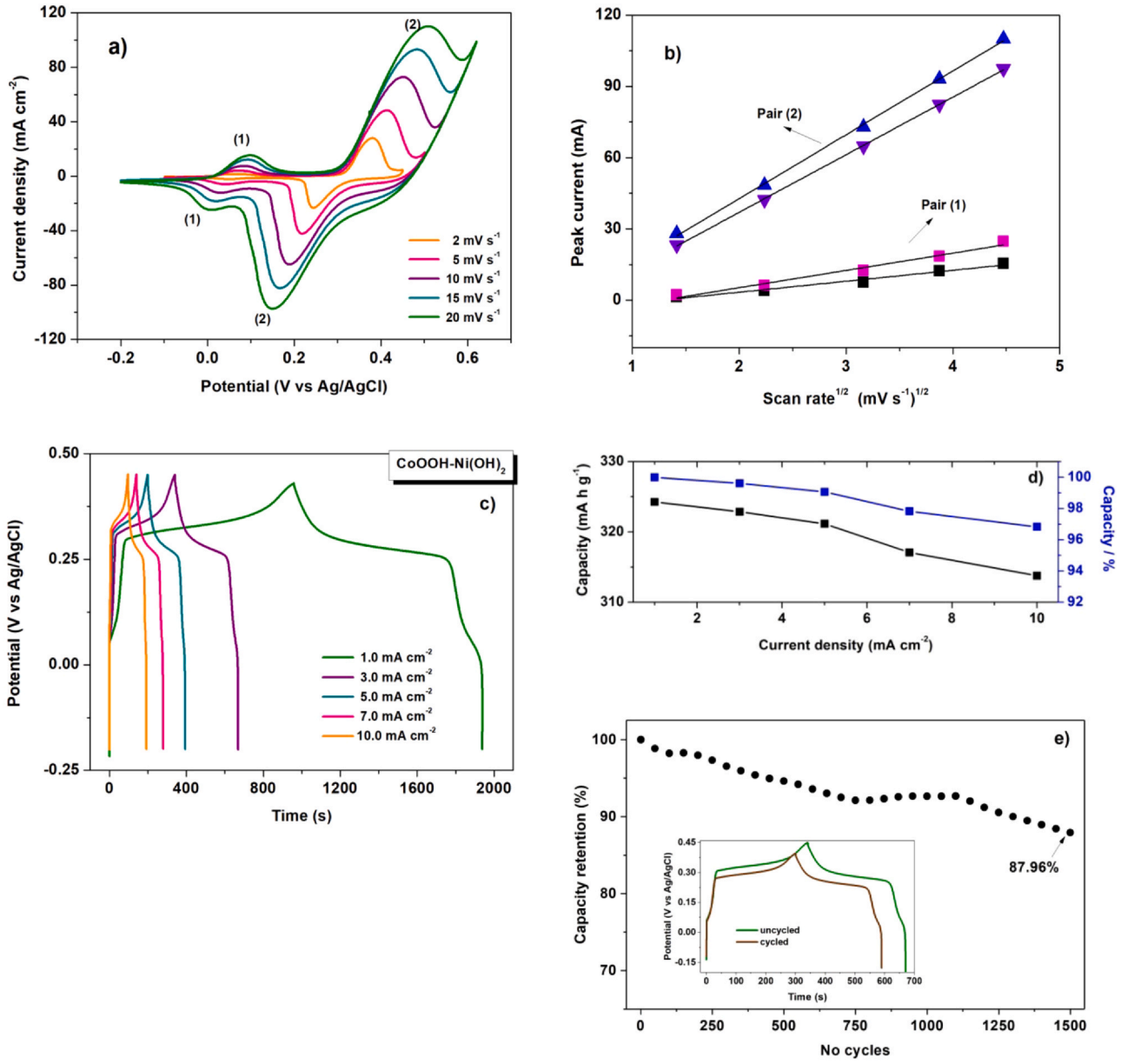

Fig. 5. (a) Cyclic Voltammogram of CoOOH/$Ni(OH)_2$ bilayers at different scan rate. (b) Dependence of the current peak with the square root of the scan rate. (c) Charge-Discharge Curves of CoOOH/$Ni(OH)_2$ bilayers. (d) corresponding Capacitance for different current densities. (e) Stability of CoOOH/$Ni(OH)_2$ as function of the number cycle.

film. Their electrochemical studies indicated that the CoOOH layer is important for the excellent electrochemical activity in the multilayer films, since it provides a large surface area for the dispersion of MnO_2 nanosheets. They also reported a capacity of 507 F g^{-1} at 0.01 mA cm^{-2}. Another interesting work was published by Li et al. [15], where a composite material was obtained by depositing Co-Ni oxyhydroxide on top of carbon nanotubes using the chemical deposition method. The composite showed a high retention capacitance of 853 F g^{-1} at 5 mV s^{-1} and 75% with a 10-fold increase in current density. Cyclic stability was 100% after 10,000 cycles of CV. More recently Nguyen et al. [1] prepared bilayer films of $Ni(OH)_2$/$Co(OH)_2$ on steel substrate by electrodeposition method. The higher electrochemical response of the films with specific capacitance of 1564 F g^{-1} at 1.0 A g^{-1} can be associated with the resulting redox reactions of the metallic species present in the lamellar films. To our knowledge, CoOOH/$Ni(OH)_2$ films obtained by the methodology proposed in this work have not been previously reported in the literature. The high value of the capacitance of the synthetized bilayer films suggests that this approach is a convenient route for the design and production of promising materials for energy storage devices. This also shows the advantages of combining the different redox chemistry of materials in the quest for a superior electrochemical response.

The EIS characterization was performed in the frequency range from 10^4 Hz to 0.01 Hz, in 10 mV amplitude, in Open Circuit Potential regime with 300 s of pretreatment to stabilize the system. Fig. 6(a) shows the Nyquist plot for the films obtained under different conditions. In the high frequency region, both films show the semicircle formation associated with charge transfer processes. As can be seen, this effect is more pronounced for $Ni(OH)_2$/CoOOH bilayers films. The charge transfer resistance (Rct) was determined using the equivalent circuit model, which is found in the inset in Fig. 6(a). The determined values are 7.56 Ω and 0.22 Ω for the $Ni(OH)_2$/CoOOH and CoOOH/$Ni(OH)_2$ films, respectively. Obviously, in $Ni(OH)_2$/CoOOH films there is a great restriction in the kinetics of the redox reaction at the electrode-electrolyte interface, resulting in a more limited electrochemical

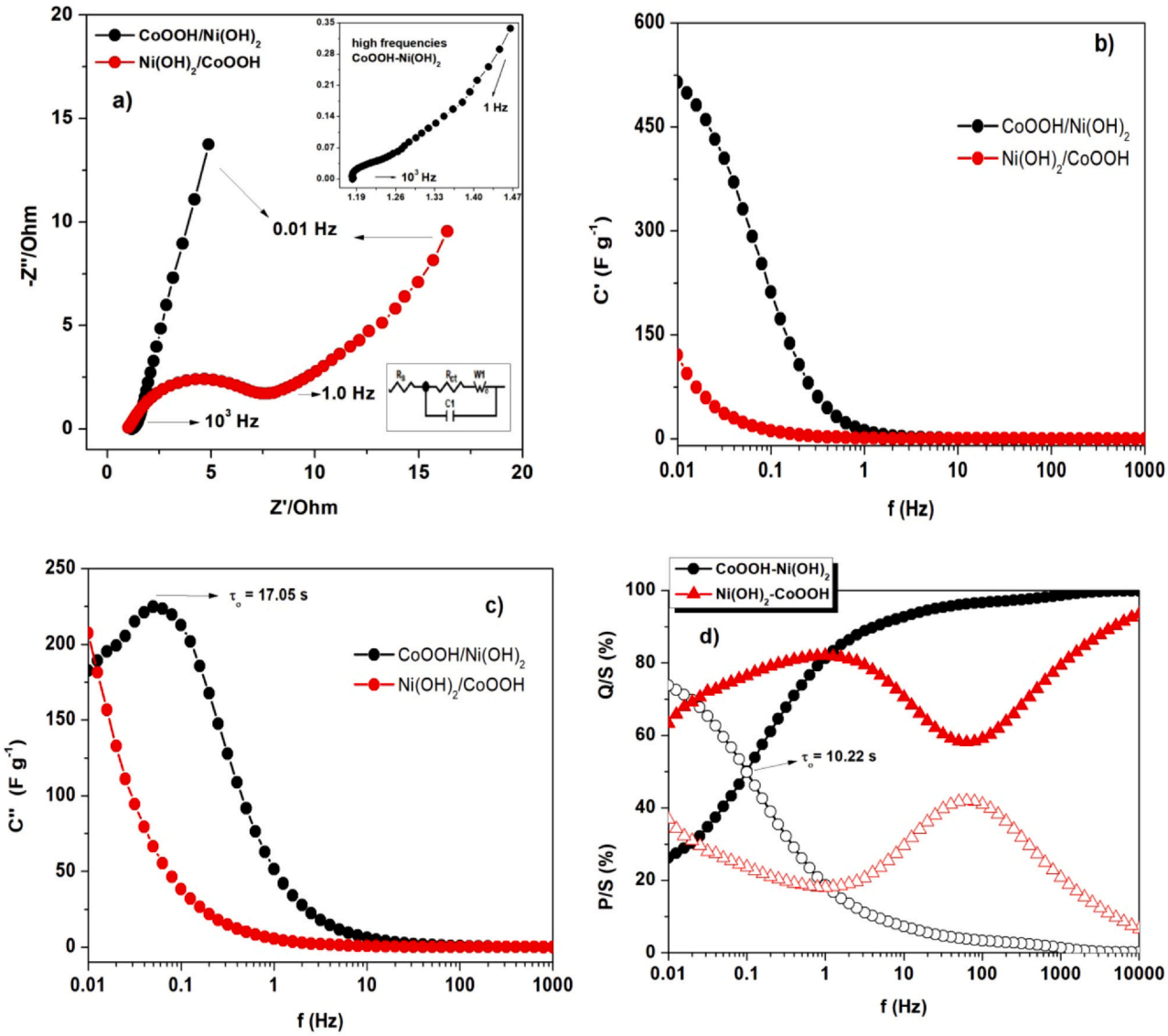

Fig. 6. (a) Nyquist plot for the $CoOOH/Ni(OH)_2$ and $Ni(OH)_2/CoOOH$ bilayer films. Inset: region of high frequencies in $CoOOH/Ni(OH)_2$ bilayers and circuit equivalent. (b) Dependence of the real and (c) imaginary capacitance with the frequency and (d) Reactive power (P/S) and active power (Q/S) normalized vs frequency, for the $CoOOH/Ni(OH)_2$ and $Ni(OH)_2/CoOOH$ films.

performance. There is also a dependence of the behavior of bilayer films with respect to the composition of the outermost layer. The responses of $Ni(OH)_2/CoOOH$ is quite similar to the single CoOOH film and conversely the $CoOOH/Ni(OH)_2$ film respond more closely to single $Ni(OH)_2$ film (Fig. S3- Supporting Information).

In the low frequency region, a line with a higher slope is formed for $CoOOH/Ni(OH)_2$ films indicating lower diffusion resistance and better capacitive behavior. For the $Ni(OH)_2/CoOOH$ films the angle of this line is approximately 45°, suggesting that in this frequency range the process is dominated by diffusion. However, the capacitive response and suitability of the material for applications in energy storage devices can be better interpreted by converting the impedance data to capacitance and complex power.

Fig. 6(b) shows the dependence of the real capacitance with the frequency for the two bilayer films. It is observed that the $CoOOH/Ni(OH)_2$ films reach the maximum value of capacitance in the low frequency region and that for 0.01 Hz the determined value was 514 F g^{-1}. In the $Ni(OH)_2/CoOOH$ films the determined value of the capacitance was 120.7 F g^{-1}.

It was also possible to determine the value of the relaxation time constant τ_o from the peak frequency in the C'' vs frequency graphic shown in Fig. 6(c). This variable is associated with ion transport and electrode performance. The time constant for the $CoOOH/Ni(OH)_2$ films is 17.05 s. On the other direction, it was not possible to determine τ_o for the $Ni(OH)_2/CoOOH$ films in this frequency range. This indicates that during the time in which the data was recorded ion diffusion and charge transfer processes were not concluded, as suggested from Nyquist graph in Fig. 6(a).

Fig. 6(d) shows the behavior of the complex power with the frequency for the two prepared bilayers. As it is possible to observe in the complex capacitance, for the $Ni(OH)_2/CoOOH$ films, in the studied frequency range they do not reach a capacitive state. In the high frequency region, the active power (resistive characteristics) dominates the power response and decreases with decreasing frequency, producing an increase in the reactive power till approximately 100 Hz. From this value the active power returns to dominate the power response and consequently, the reactive power decreases without interception between the curves. Under these

conditions, the films do not reach the maximum performance and it is also not possible to calculate τ_o.

For CoOOH/ $Ni(OH)_2$ bilayers films, the active power dominates the response at high frequencies values and decrease as the frequency decrease. The opposite trend is observed for the reactive power or capacitive character, which increases with decreasing frequency. The curves intercept corresponds to the optimum point of operation where the electrodes release stored energy and power more efficiently. From the frequency at which the intercept occurs (approximately 0.1 Hz), the τ_o value can be calculated. The obtained value is 10.22 s. It can also be emphasized that at 0.01 Hz the electrodes have a capacitive response of 75%, which is highly suitable for applications in energy storage devices.

4. Conclusions

A new $Ni(OH)_2$/CoOOH bilayer film architecture was successfully prepared from the electrodeposition method on steel substrate. The techniques of X-ray diffraction and Raman spectroscopy confirmed the formation of the CoOOH / Ni $(OH)_2$ phase by using electrodeposition preparation method.

Bilayers films with $Ni(OH)_2$ deposited on CoOOH (CoOOH/$Ni(OH)_2$) showed higher values of specific capacitance of 324.27 mA h g^{-1} at 1.0 mA cm^{-2}. For 10 mA cm^{-2}, high capacitance retention of 96.82% was achieved, indicating good charge storage capacity at higher charge-discharge rates. These films also showed low time constant of 17.05 s. These results may be associated with the direct growth of CoOOH films on the substrate, without the use of additives or complexing agents, which favors good conductivity. Moreover, CoOOH/$Ni(OH)_2$ bilayers lead to an increase in the redox active sites, allowing a greater diffusion of electroactive species and thus holding a rapid transfer of ions.

CRediT authorship contribution statement

The authors have met the ethical requirements of Elsevier. Thus we declare that the present work has not been published (neither totally, nor partially) previously and that its publication in another place is not being considered. We also declare that all authors approve the publication of the work, as well as the authorities responsible for the entities where it was developed. If accepted for publication, it will not be published elsewhere in English or in any other language, without the written consent of the publisher. Finally, we declare that all authors had an important contribution in this paper.

Declaration of Competing Interest

The authors declare that they have no known competing financial interests or personal relationships that could have appeared to influence the work reported in this paper.

Acknowledgment

The authors would like to thank FAPEAM contract number 062.00939/2019, and FCT Portuguese agencies for the financial support. This study was financed in part by the Coordenação de Aperfeiçoamento de Pessoal de Nível Superior - Brasil (CAPES) - Finance Code 001.

Appendix A. Supporting information

Supplementary data associated with this article can be found in the online version at doi:10.1016/j.jallcom.2021.159858.

References

[1] T. Nguyen, M. Boudard, M.J. Carmezim, M.F. Montemor, Layered $Ni(OH)_2$-Co $(OH)_2$ films prepared by electrodeposition as charge storage electrodes for hybrid supercapacitors, Sci. Rep. 7 (2017) 39980.
[2] X. Li, Z. Song, W. Guo, Y. Wang, M. Liang, P. Jiang, Vertically porous $Ni(OH)_2$/Ni thin film on carbon cloth for high performance flexible supercapacitors, Mater. Lett. 190 (2017) 20–23.
[3] J. Zhang, Y. Liu, H. Guan, Y. Zhao, B. Zhang, Decoration of nickel hydroxide nanoparticles onto polypyrrole nanotubes with enhanced electrochemical performance for supercapacitors, J. Alloy. Compd. 721 (2017) 731–740.
[4] L. Aguilera, Y. Leyet, R. Peña-Garcia, E. Padrón-Hernández, R.R. Passos, L.A. Pocrifka, Cabbage-like α-$Ni(OH)_2$ with a good long-term cycling stability and high electrochemical performances for supercapacitor applications, Chem. Phys. Lett. 677 (2017) 75–79.
[5] V. Augustyn, P. Simon, B. Dunn, Pseudocapacitive oxide materials for high-rate electrochemical energy storage, Energy Environ. Sci. 7 (2014) 1597.
[6] L. Aguilera, Y. Leyet, E. Padrón-Hernández, R.R. Passos, L.A. Pocrifka, Understanding electrochemical performance of $Ni(OH)_2$ films:a study contributions to energy storage, J. Solid State Electrochem. 22 (2018) 1621–1628.
[7] A. Le Comte, T. Brousse, D. Bélanger, New generation of hybrid carbon/$Ni(OH)_2$ electrochemical capacitor using functionalized carbon electrode, J. Power Sources 326 (2016) 702–710.
[8] L. Aguilera, P. Aguiar, Y. Leyet, E. Padrón-Hernández, R.R. Passos, L. Pocrifka, Morphology and performance of CoOOH films synthesized via electrochemical oxidation: substrate effects, J. Solid State Electrochem. 22 (2018) 3845–3852.
[9] F. Barde, M.-R. Palacin, B. Beaudoin, A. Delahaye-Vidal, J.M. Tarascon, New approaches for synthesizing γIII-CoOOH by soft chemistry, Chem. Mater. 16 (2004) 299–306.
[10] A.D. Jagadale, V.S. Kumbhar, D.S. Dhawale, C.D. Lokhande, Performance evaluation of symmetric supercapacitor based on cobalt hydroxide [$Co(OH)_2$] thin film electrodes, Electrochim. Acta 98 (2013) 32–38.
[11] L. Peng, L. Lv, H. Wan, Y. Ruan, X. Ji, J. Liu, L. Miao, C. Wang, J. Jiang, Understanding the electrochemical activation behavior of $Co(OH)_2$ nanotubes during the ion-exchange process, Mater. Today Energy 4 (2017) 122–131.
[12] W. Wen, D. Liang, J.-P. Cheng, J.-M. Wu, CoOOH ultrafine nanoparticles for supercapacitors, RSC Adv. 6 (2016) 70947–70951.
[13] M. Wang, W. Ren, Y. Zhao, H. Cui, Synthesis of nanostructured CoOOH film with high electrochemical performance for application in supercapacitor, J. Nanopart. Res. 16 (2014) 2181.
[14] H. Zheng, F. Tang, M. Lim, A. Mukherji, X. Yan, L. Wang, M. Lu, Multilayered films of cobalt oxyhydroxide nanowires / manganese oxide nanosheets for electrochemical capacitor, J. Power Sources 195 (2010) 680–683.
[15] M. Li, J.P. Cheng, F. Liu, X.B. Zhang, In situ growth of nickel-cobalt oxyhydroxide / oxide on carbon nanotubes for high performance supercapacitors, Electrochim. Acta 178 (2015) 439–446.
[16] Y. Wu, H. Chen, Y. Lu, J. Yang, X. Zhu, Y. Zheng, G. Lou, Y. Wu, Q. Wu, Z. Shen, Z. Pan, Rational design of cobalt–nickel double hydroxides for flexible asymmetric supercapacitor with improved electrochemical performance, J. Colloid Interface Sci. 581 (2021) 455–464.
[17] J. Cao, Q. Mei, R. Wu, W. Wang, Flower-like nickel–cobalt layered hydroxide nanostructures for super long-life asymmetrical supercapacitors, Electrochim. Acta 321 (2019) 134711.
[18] H. Zuo, W. Fu, R. Fan, D. Dastan, H. Wang, Z. Shi, Bilayer carbon nanowires/nickel cobalt hydroxides nanostructures for high-performance supercapacitors, Mater. Lett. 263 (2020) 127217.
[19] J. Yang, H. Liu, W.N. Martens, R.L. Frost, Synthesis and characterization of Cobalt hydroxide, cobalt oxyhydroxide, and cobalt oxide nanodiscs, J. Phys. Chem. C 114 (2010) 111–119.
[20] C.W. Tang, C.B. Wang, S.H. Chien, Characterization of cobalt oxides studied by FT-IR, Raman, TPR and TG-MSC, Thermochim. Acta 473 (2008) 68–73.
[21] D.S. Hall, D.J. Lockwood, S. Poirier, C. Bock, B.R. MacDougall, Raman and infrared spectroscopy of α and β phases of thin nickel hydroxide films electrochemically formed on nickel, J. Phys. Chem. A 116 (2012) 6771–6784.
[22] T. Nguyen, M. Boudard, M. Joa, $Ni_xCo_{1-x}(OH)_2$ nanosheets on carbon nanofoam paper as high areal capacity electrodes for hybrid supercapacitors, Energy 126 (2017) 208–216.
[23] S.R. Shieh, T.S. Duffy, Raman spectroscopy of $(Co(OH)_2)$ at high pressures: implications for amorphization and hydrogen repulsion, Phys. Rev. B - Condens. Matter Mater. Phys. 66 (2002) 1–8.
[24] Y.C. Liu, J.A. Koza, J.A. Switzer, Conversion of electrodeposited $Co(OH)_2$ to CoOOH and Co_3O_4, and comparison of their catalytic activity for the oxygen evolution reaction, Electrochim. Acta 140 (2014) 359–365.